

# Production of orbitally excited vector mesons in diffractive DIS

F. Caporale<sup>1</sup>, I.P. Ivanov<sup>1,2</sup>

<sup>1</sup> INFN, Gruppo Collegato di Cosenza, Italy

<sup>2</sup> Sobolev Institute of Mathematics, Novosibirsk, Russia

## Abstract

Within the  $k_t$ -factorization framework, we study diffractive production of orbitally excited vector mesons and compare it with the production of radial excitations, focusing on the  $\rho(1450)/\rho(1700)$  case. At small  $Q^2$ , orbital excitation of light quarkonia is found to dominate over radial excitations in diffractive production. We predict strong suppression of the production of orbital excitations by longitudinal photons, which leads to very small  $\sigma_L/\sigma_T$  ratio. At small  $Q^2$ , the  $s$ -channel helicity violating transitions contribute  $\sim 10$ – $15$  % of the transverse cross section and  $\sim 50\%$  of the longitudinal cross section. We also study mixing between radial and orbital excitations and determine strategies towards clarification of  $S$ -wave/ $D$ -wave assignment to  $\rho(1450)$  and  $\rho(1700)$  mesons. The results are compared with the experimental data available, and predictions for future experiments are given.

## 1 Introduction

Diffractive production of vector mesons (VM) in DIS  $\gamma^*p \rightarrow Vp$  ( $V = \rho, \phi, J/\psi$  etc.) is a very active field of research (see recent review [1] and references therein). So far, the main focus has been on the ground state mesons, while diffractive production of excited states has not enjoyed much attention. Perhaps, the most studied case so far was the production of radially excited charmonium  $J/\psi(2S)$ , where remarkable consequences of the presence of a node in the radial wave function [2] were nicely confirmed by H1 measurements [3].

Experimental studies of excited  $\rho'$  production should be even more rewarding. First, production of excited mesons probes the dipole cross section at larger dipole sizes than the production of ground states, see e.g. analysis of  $\rho'/\rho''$  in [4] and the recent study of  $\rho_3$  in [5]. Such sensitivity to soft diffraction can help understand the phenomenon of saturation, [6]. Besides, it is expected that diffractive production of  $\rho'$  can help resolve the long standing puzzle of the radial/orbital excitation assignment to the  $\rho(1450)$  and  $\rho(1700)$  mesons<sup>1</sup>, see [7].

Diffractive production of excited  $\rho'$  mesons has been observed in a number of fixed target experiments with relatively high energies. Diffractive production of  $\rho'(1600)$  was reported in  $\pi^+\pi^-$  [8] and  $4\pi$  [9] final states (for reanalysis of these data in terms of  $\rho(1450)$  and  $\rho(1700)$

---

<sup>1</sup>In his analysis of  $\rho(1450)$  and  $\rho(1700)$  mesons, the author of [7] concludes that "The way forward with  $1^{--} q\bar{q}$  states is to study diffractive dissociation of the photon".

mesons see [10]). These states were also studied in the Fermilab experiment E687 [11] both in  $2\pi$  and  $4\pi$  channels. In addition, there are indications that the  $\rho(1700)$  — which is believed to be predominantly the orbital excitation — can play essential role in an interesting narrow dip structure observed by E687 in the  $6\pi$  final state [12]. However, all these experiments gave only the value of the photoproduction cross section, and neither energy or  $Q^2$  dependence, nor helicity structure of the reaction was studied. This gap was partially filled by the H1 measurement of  $\rho'$  electroproduction at  $4 < Q^2 < 50 \text{ GeV}^2$  [13], but due to low statistics the results presented had large errorbars.

In theory, production of orbitally excited vector mesons is expected to be suppressed by Fermi motion, as its radial wave function vanishes at the origin. This suppression was believed to be sufficiently strong and even prompted the authors of [4] to consider diffractive  $\rho(1450)$  and  $\rho(1700)$  production neglecting in both cases the  $D$ -wave contributions altogether. Only in [14] were the  $S$ -wave and  $D$ -wave vector meson production amplitudes calculated within the  $k_t$ -factorization approach, and the first estimates [15] showed that at small-to-moderate  $Q^2$  the production rates of the  $D$ -wave and  $2S$   $\rho'$  states were roughly of the same order.

In this paper we extend this research and report more detailed numerical results on  $D$ -wave vector meson production.

## 2 Amplitude of the vector meson production

We use the usual notation for kinematical variables.  $Q^2$  is the photon's virtuality,  $W$  is the total center-of-mass energy of the  $\gamma^*p$  collision. The momentum transfer from proton to photon is denoted by  $\Delta_\mu$  and at high energies is almost purely transverse:  $-\Delta^2 = |t| \approx |t'| = \vec{\Delta}^2$ . The transverse vectors (orthogonal to the  $\gamma^*p$  collision axis) will be always labelled by an arrow.

Diffractive production of meson  $V$  with mass  $m_V$  can be treated in the lowest Fock state approximation as production of the  $q\bar{q}$  pair of invariant mass  $M \neq m_V$ , which is then projected, at the amplitude level, onto the final state. Within the leading  $\log_x^1$  accuracy the higher Fock states are reabsorbed into the evolution of the unintegrated gluon density (or color dipole cross section). A typical amplitude contains the valence quark loop, with integration over the quark transverse momentum  $\vec{k}$  and its fraction of photon's lightcone momentum  $z$ , and the uppermost gluon loop, with the integration over transverse momentum  $\vec{\kappa}$ .

Throughout the text, the ground state vector mesons (always understood as  $1S$  states) will be generically labelled by  $V$  or  $V_{1S}$ , their radial excitations will be labelled by  $V_{2S}$ , while the pure  $D$ -wave vector mesons will be labelled by  $V_D$ .

A generic form of the helicity amplitudes  $\gamma^*(\lambda_\gamma) \rightarrow V_D(\lambda_V)$  is

$$ImA_{\lambda_V;\lambda_\gamma} = \frac{c_V \sqrt{4\pi\alpha_{em}}}{4\pi^2} \int \frac{dz d^2\vec{k}}{z(1-z)} \int \frac{d^2\vec{\kappa}}{\vec{\kappa}^4} \alpha_s \mathcal{F}(x_1, x_2, \vec{\kappa}, \vec{\Delta}) \cdot I(\lambda_\gamma \rightarrow \lambda_V) \cdot \psi_D(\mathbf{p}^2). \quad (1)$$

Here  $c_V$  is the flavor-dependent average charge of the quark, the argument of the strong coupling constant  $\alpha_s$  is  $\max[z(1-z)(Q^2 + M^2), \vec{\kappa}^2]$ . The radial wave function of the vector meson depends on the spherically symmetric quantity  $\mathbf{p}^2$ , where  $\mathbf{p}$  is the relative  $q\bar{q}$  momentum written in the  $q\bar{q}$  rest frame.  $\mathcal{F}(x_1, x_2, \vec{\kappa}, \vec{\Delta})$  is the skewed unintegrated gluon distribution, with  $x_1 \neq x_2$  being the fractions of the proton's momentum carried by the uppermost gluons. The appearance of skewed (or generalized) parton distributions is characteristic for scattering processes that change the mass/virtuality of the projectile [16, 17]. In the  $k_t$ -factorization

approach, the skewness is transferred to the unintegrated distributions. The real part of the amplitude can be reconstructed from the imaginary part (1) using analyticity.

The twist analysis of helicity amplitudes (1) was performed in [14]. The principal findings were: (1) the longitudinal cross section was found to be particularly suppressed in comparison with  $S$ -wave meson production, which translated into abnormally small  $\sigma_L/\sigma_T$  ratio, and (2) the  $s$ -channel helicity non-conserving (SCHNC) amplitudes played much more important role than in the case of  $\rho$ . A comparison of  $V_D$  and the spin-3 ground state of the same quarkonium  $V_3$  performed in [5] offered an insight into smallness of  $\sigma_L(V_D)$  in terms of Clebsch-Gordan coefficients.

### 3 Numerical results

Here we present numerical results for the most interesting case of  $\rho_D$ , which in this section we identify with the physical state  $\rho(1700)$ .

In order to integrate (1) numerically, one needs to specify models for the off-forward unintegrated gluon density and for the vector meson wave function. The former was related to the forward unintegrated gluon density, see [1], whose parametrizations were borrowed from [18]. The choice of a particular parametrization affects the numerical results only marginally. For the vector meson wave function we used the appropriately normalized Gaussian Ansatz. The particular choice of the radial wave function changes sizably only the overall normalization of the predicted cross sections, but not their shapes. The experimental value of the leptonic decay width  $\Gamma(\rho(1700) \rightarrow e^+e^-)$ , which was used to fix the size parameter of the wave function, is known very poorly, which significantly affects the accuracy of our predictions. Below, we show numerical results using  $\Gamma(\rho(1700) \rightarrow e^+e^-) = 0.14\text{--}0.7$  keV. Below, we also show for comparison the cross sections of  $\rho$  and  $\rho_{2S}$  production. In both cases, we varied the corresponding leptonic decay widths  $\Gamma = (1 \div 3)\Gamma_{\text{PDG}}$  to roughly control the uncertainty of numerical results.

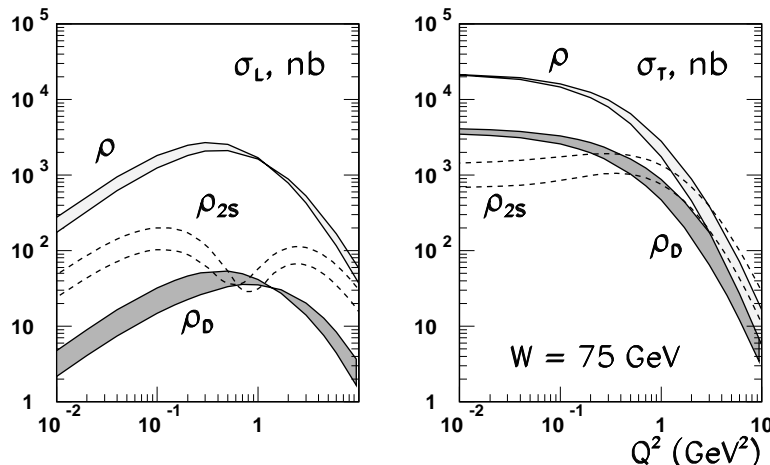


Figure 1: The  $Q^2$ -dependence of the longitudinal (left plot) and transverse (right plot)  $\rho_D$  production cross sections (dark shade regions). For comparison, we also show our results for the  $\rho$  (light shaded regions) and  $\rho_{2S}$  (dashed curves). The shaded regions show the sensitivity of the results to the variation of the leptonic decay width.

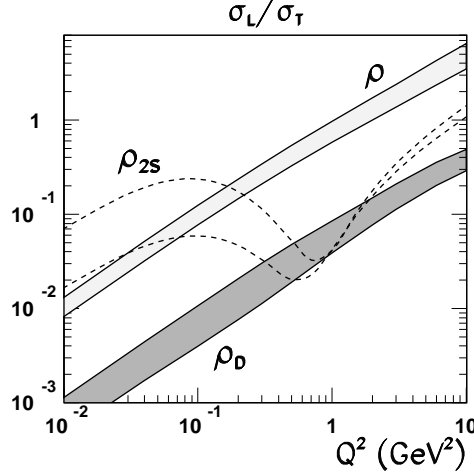


Figure 2: The  $Q^2$ -dependence of  $R = \sigma_L/\sigma_T$  ratio for  $\rho_D$ ,  $\rho$  and  $\rho_{2S}$ . Notation is the same as in Fig. 1.

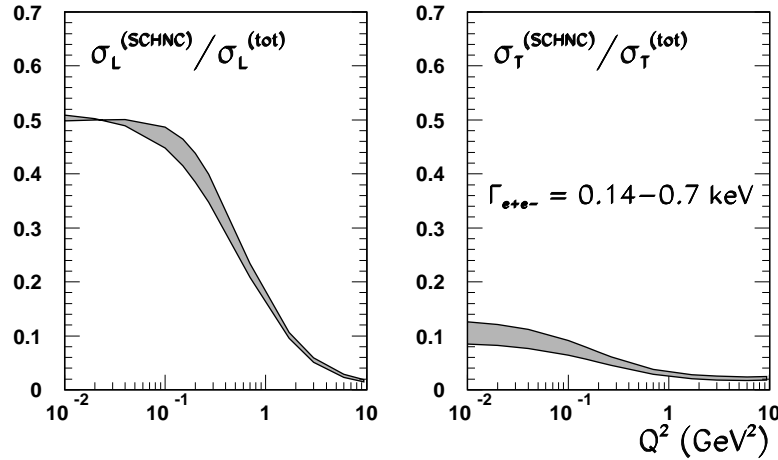


Figure 3: The relative weight of the  $s$ -channel helicity non-conserving contributions to longitudinal (left plot) and transverse (right plot)  $\rho_D$  production cross sections as functions of  $Q^2$ . The shaded regions correspond to  $\Gamma(\rho(1700) \rightarrow e^+e^-) = 0.14\text{--}0.7$  keV.

In Fig. 1 we show the longitudinal and transverse cross sections for  $\rho_D$  as well as for  $\rho$  and  $\rho_{2S}$ . At the photoproduction point,  $\sigma_T(\rho_D)/\sigma_T(\rho) \approx 0.2$ , and it increases slightly towards higher  $Q^2$ . The cross section of  $\rho_D$  production by longitudinal photons is always small,  $\sigma_L(\rho_D)/\sigma_L(\rho) \sim 0.01\text{--}0.03$ , in agreement with qualitative studies [14]. This translates into anomalously small longitudinal-to-transverse ratio  $R(\rho_D) \equiv \sigma_L(\rho_D)/\sigma_T(\rho_D) \sim 0.1R(\rho)$ , which is illustrated by Fig. 2.

Note that the  $\rho_{2S}$  production cross sections show very different patterns of  $Q^2$  behavior, see Fig. 1 and Fig. 2. Comparison of  $\sigma(\rho_{2S})$  and  $\sigma(\rho_D)$  shows that at small  $Q^2$ , and in particular, at the photoproduction point,  $\rho_D$  should dominate over  $\rho_{2S}$ . At moderate  $Q^2 \sim 1$  GeV<sup>2</sup> both mesons are expected to be produced at comparable rates, and at  $Q^2 \gtrsim 5$  GeV<sup>2</sup> the  $\rho_{2S}$  production should take over.

Fig. 3 demonstrates the role of SCHNC transitions in  $\rho_D$  production. In accordance with expectations, at small  $Q^2$  the  $s$ -channel helicity violating amplitudes generate a sizable portion of both longitudinal and transverse cross sections. As  $Q^2$  grows, the SCHNC effects gradually die out, however, their magnitude is still larger than SCHNC observed in production of ground state  $\rho$  mesons [19]. At small  $Q^2$ , the presence of strong helicity violating amplitudes noticeably modifies the  $t$ -dependence of the differential cross sections at  $|t| \gtrsim 0.3 \text{ GeV}^2$ .

We also checked the energy dependence of the  $\rho_D$  production cross section, which can be conveniently parametrized with simple power law,  $\sigma(W) \propto W^\delta$ . We checked the  $Q^2$  behavior of the exponent  $\delta$  and found it somewhat smaller than the corresponding exponent for  $\rho$  production. This can be traced back to the larger color dipole sizes probed in  $\rho_D$  production and to the enhanced contribution from larger  $|t|$  region, although the effect is not as dramatic as in the case of spin-3 meson production, see [5].

## 4 Testing purity of the $D$ -wave

If the  $\rho(1450)$  and  $\rho(1700)$  were well separated eigenstates of the  $q\bar{q}$  angular momentum, then using  $Q^2$  behavior of their diffractive production cross sections, Fig. 1, one could easily tell radial from orbital excitation. In reality one has to account for a possibly strong mixing between the radial and orbital excitations as well as for their significant overlapping. The legitimate question is whether diffractive production can be used under these circumstances to probe the structure of  $\rho(1450)$  and  $\rho(1700)$ . Analysis of this type was conducted in [4], where authors considered both  $\rho(1450)$  and  $\rho(1700)$  as states composed of a pure  $2S$  and of anything else (orbital excitation, hybrid etc.). They determined the mixing angle to be  $\theta = 41.2^\circ$ , and were able to describe the scarce experimental data available. With too many assumptions ( $\sigma(\rho_D) = 0$ , strict SCHC etc.) and poorly known parameters, the precision of the results obtained in [4] seems to us doubtful.

We agree with [4] that one should study not  $\rho(1450)$  and  $\rho(1700)$  separately but  $\pi^+\pi^-$  or  $4\pi$  final state in the entire region of multipion invariant mass  $M = 1.2\text{--}1.8 \text{ GeV}$ . In our opinion, two quantities are particularly useful for determination of the internal structure of  $\rho(1450)$  and  $\rho(1700)$ : (i) the  $Q^2$  variations of the invariant mass shape, and (ii) the level of  $s$ -channel helicity violation. Both quantities should be studied in the region of small-to-moderate  $Q^2$ , precisely where the  $\rho(2S)$  cross section is expected to have strong variations due to the node effect.

We consider simple  $2S/D$ -wave mixing in the  $\rho$  system and represent the two  $\rho'$  states as

$$|\rho(1450)\rangle = \cos\phi|2S\rangle + \sin\phi|D\rangle, \quad |\rho(1700)\rangle = -\sin\phi|2S\rangle + \cos\phi|D\rangle. \quad (2)$$

The total amplitude for a give final state  $f = 2\pi, 4\pi$  with invariant mass  $M_f$  is written as

$$A = A_\rho D_\rho(M_f) + A_{\rho(1450)} D_{\rho(1450)}(M_f) + A_{\rho(1700)} D_{\rho(1700)}(M_f), \quad (3)$$

where  $A_i$  are the production amplitudes of each resonance calculated within the same approach and  $D_i$  are the corresponding Breit-Wigner factors. In Fig. 4 we show typical invariant mass spectra of the  $4\pi$  states for  $Q^2 = 0$  and  $Q^2 = 1 \text{ GeV}^2$ . The solid curves correspond to no mixing, while dashed and dotted curves correspond to  $\phi = \pi/4$  and  $\phi = -\pi/4$ . The  $M_{4\pi}$ -shape at fixed  $Q^2$  and its variation with  $Q^2$  growth show interesting dependence on the mixing angle.

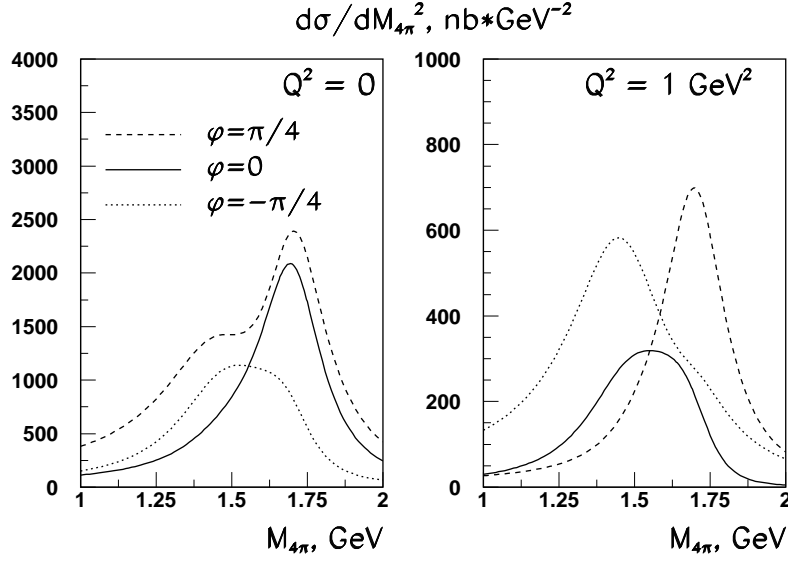


Figure 4: Typical  $M_{4\pi}$  dependence of diffractive  $4\pi$  production cross section in case of several values of mixing angle and for two values of photon virtuality:  $Q^2 = 0$  (left plot) and  $Q^2 = 1$   $\text{GeV}^2$  (right plot).

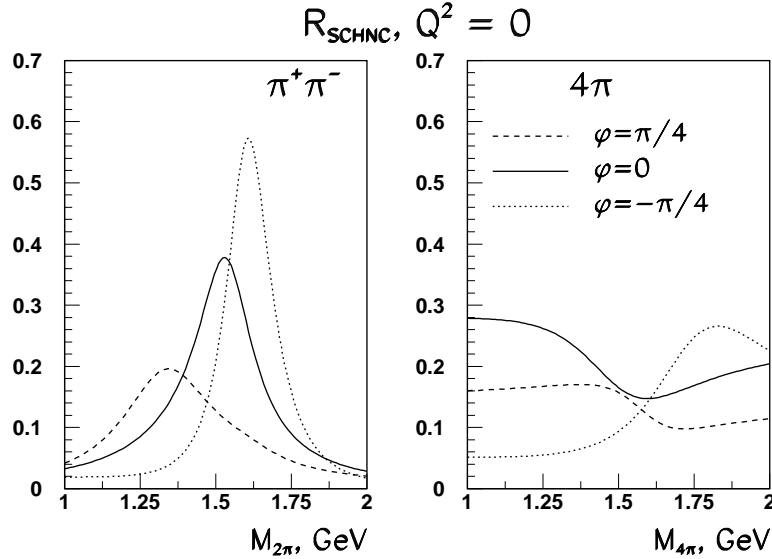


Figure 5: The fractions of SCHNC contribution  $R_{\text{SCHNC}}$  to the diffractive  $\pi^+\pi^-$  (left plot) and  $4\pi$  (right plot) photoproduction as functions of the final state invariant mass. On each plot, three different curves shown correspond to no  $2S/D$  mixing (solid lines), mixing with  $\phi = \pi/4$  (dashed lines) and mixing with  $\phi = -\pi/4$  (dotted lines).

Another way to separate radial/orbital excitations is to study the magnitude of the  $s$ -channel helicity non-conservation  $R_{\text{SCHNC}} = 1 - \sigma(\text{SCHC})/\sigma(\text{full})$  as a function of the final state invariant mass  $M_f$ . Although at the photoproduction point both  $\rho_{2S}$  and  $\rho_D$  have

roughly  $\sim 10\text{--}15\%$  of their cross sections coming from SCHNC amplitudes, their interference pattern is sensitive to the mixing. Fig. 5 shows values of  $R_{\text{SCHNC}}$  in the cases of  $\pi^+\pi^-$  (left plot) and  $4\pi$  (right plot) final states in the photoproduction limit. For these plots, we took  $Br(\rho(1450) \rightarrow \pi^+\pi^-) = Br(\rho(1700) \rightarrow \pi^+\pi^-) = 0.2$ . In the  $\pi^+\pi^-$  case, the helicity violating amplitudes come from excited states, while the helicity conserving amplitudes have a non-trivial interference between  $\rho$  and excited states. This produces a peak in  $R_{\text{SCHNC}}(M_{2\pi})$  plot, whose position is sensitive to the mixing angle. In the  $4\pi$  final state, there is no  $\rho$  contribution, and the SCHNC is substantial throughout the whole  $M_{4\pi}$  region shown, its interference pattern again sensitive to the mixing. We underline that Figs. 4, 5 show only typical patterns to look for. Exact predictions are difficult due to too many poorly known parameters in the game.

## 5 Comparison with experimental data and future possibilities

In 1980's the Omega Collaboration has studied diffractive photoproduction of  $\rho'(1600)$  meson in  $\pi^+\pi^-$  and  $4\pi$  channels. From the published results  $\sigma(\rho' \rightarrow \pi^+\pi^-)/\sigma(\rho) = 0.01 \pm 0.002$  [8] and  $\sigma(\rho' \rightarrow 4\pi) = 0.7 \pm 0.2 \mu\text{b}$  [9] one can estimate the  $\rho'(1600)$  photoproduction cross section as roughly  $1 \mu\text{b}$ . Although these results were reanalyzed in [10] in terms of two excited states  $\rho(1450)$  and  $\rho(1700)$ , we find it more secure to compare our results with the original data.

As shown on Fig. 1, our predictions for the photoproduction cross sections are  $\sigma(\rho_{2S}) \sim 4 \mu\text{b}$ ,  $\sigma(\rho_D) \sim 1 \mu\text{b}$ . However, since  $\rho(1450)$  and  $\rho(1700)$  are broad interfering peaks, the integration of  $d\sigma/dM_{4\pi}$  within the region  $M_{4\pi} = 1.2\text{--}1.8 \text{ GeV}$  yields  $\sigma(\rho(1450) + \rho(1700)) \sim 1.5\text{--}3 \mu\text{b}$ , depending on the  $2S/D$  mixing angle, which is not far from experiment.

As discussed above, detailed studies of the  $2\pi$  or  $4\pi$  mass spectrum, in particular, the level of  $s$ -channel helicity violation, can help resolve the  $S/D$ -wave structure of the  $\rho(1450)$  and  $\rho(1700)$ . Extraction of SCHNC amplitudes relies on reconstruction of the angular distribution of the final multipion state. For the  $\pi^+\pi^-$  state this procedure was described in [20], while for the  $4\pi$  state more analysis in the spirit of [9] should be done. Note that the conclusion made in the latter paper that at least half of all  $4\pi$  events under the peak come from an SCHC mechanism does not contradict the results of our calculations.

When extracting  $\rho'$  from the multipion final states, one must subtract from the data the  $\rho_3(1690)$  contribution, which is not negligible and which is predicted to have extremely large SCHNC contributions, see [5]. Such a separation would be possible if one either performs the full partial wave analysis, which is more suitable for the  $\pi^+\pi^-$  final state, or extracts a specific signal in the multipion final states, like  $\rho_3 \rightarrow a_2(1320)\pi \rightarrow \eta\pi^+\pi^-$ .

We also briefly comment on the recent observation by Focus Experiment [21] of a very statistically significant enhancement in the diffractive photoproduction of  $K^+K^-$  pairs at  $M_{KK} = 1750 \text{ MeV}$ . The experiment ruled out the possibility to explain this enhancement with  $\phi(1680)$  meson, which is believed to be mainly  $2S$  excitation of  $\phi$ . One could speculate if this new resonance could be the orbitally excited  $\phi$  meson. If so, our calculations predict the photoproduction cross section  $\sigma(\phi_D) \sim 200\text{--}300 \text{ nb}$ , which is  $\sim 1/5$  of the  $\phi$  photoproduction cross section calculated in the same model. Unfortunately, the experimental paper does not give the measurement results for the cross section.

## 6 Conclusions

In this paper we considered diffractive production of orbitally excited vector mesons in DIS, with a major focus on the  $D$ -wave  $\rho'$  state. The calculations were performed within the  $k_t$ -factorization framework. Although the predictions for the absolute values of the cross sections are plagued by large uncertainties of the input parameters, we find that several qualitative conclusions are stable:

- The  $\rho_D$  production cross section is roughly an order of magnitude smaller than the  $\rho$  production cross section. At small  $Q^2$ ,  $\sigma(\rho_D)$  is larger than  $\sigma(\rho_{2S})$ , casting doubt on the relevance of  $\sigma(\rho_D) = 0$  assumption used in [4].
- Studying  $\sigma_L$  and  $\sigma_T$  separately, we observe strong suppression of the longitudinal cross section, which translates into very small ratio of  $R = \sigma_L/\sigma_T$ , as was anticipated in [14].
- The role of the  $s$ -channel helicity violation is more important in  $D$ -wave state production than in the ground state production, especially at small  $Q^2$ .

Besides, our results confirm general expectations that the experimental study of diffractive multipion production in the invariant mass region of  $\rho(1450)/\rho(1700)$  interference can be a key to the  $2S$ -wave/ $D$ -wave assignment to these two mesons. Study of the  $Q^2$  variation of  $M_{4\pi}$  shapes of the cross section as well as checking the level of  $s$ -channel helicity violation should be of much help.

The work of I.P.I. is supported by the INFN Fellowship, and partly by INTAS and grants RFBR 05-02-16211 and NSh-2339.2003.2.

## References

- [1] I. P. Ivanov, N. N. Nikolaev and A. A. Savin, hep-ph/0501034.
- [2] J. Nemchik, et al, J. Exp. Theor. Phys. **86** (1998) 1054 [Zh. Eksp. Teor. Fiz. **113** (1998) 1930]; J. Nemchik, et al, Z. Phys. C **75** (1997) 71; Phys. Lett. B **339** (1994) 194.
- [3] C. Adloff *et al.*, Phys. Lett. B **541** (2002) 251; Phys. Lett. B **421** (1998) 385.
- [4] G. Kulzinger, H. G. Dosch and H. J. Pirner, Eur. Phys. J. C **7**, 73 (1999).
- [5] F. Caporale and I. P. Ivanov, arXiv:hep-ph/0504139.
- [6] K. Golec-Biernat, Acta Phys. Polon. B **35** (2004) 3103.
- [7] D. V. Bugg, Phys. Rept. **397**, 257 (2004).
- [8] D. Aston *et al.*, Phys. Lett. B **92** (1980) 215.
- [9] D. Aston *et al.*, Nucl. Phys. B **189** (1981) 15; M. Atkinson *et al.* [Omega Photon Collaboration], Phys. Lett. B **108** (1982) 55; Z. Phys. C **26** (1985) 499.
- [10] A. Donnachie and H. Mirzaie, Z. Phys. C **33** (1987) 407.



- [11] P. Lebrun [E687 Collaboration], FERMILAB-CONF-97-387-E, *talk given at the 7th International Conference on Hadron Spectroscopy (Hadron 97), Upton, NY, 25-30 Aug 1997.*
- [12] P. L. Frabetti *et al.* [E687 Collaboration], Phys. Lett. B **514** (2001) 240; P. L. Frabetti *et al.*, Phys. Lett. B **578** (2004) 290.
- [13] H1 collaboration, paper pa01-088, submitted to ICHEP 96, Warsaw 1996 (Poland).
- [14] I. P. Ivanov and N. N. Nikolaev, JETP Lett. **69** (1999) 294.
- [15] I. P. Ivanov, PhD thesis, arXiv:hep-ph/0303053.
- [16] A. V. Radyushkin, Phys. Lett. B **385** (1996) 333; Phys. Rev. D **56** (1997) 5524; X. D. Ji, Phys. Rev. D **55** (1997) 7114; A. V. Belitsky and A. V. Radyushkin, arXiv:hep-ph/0504030; M. Diehl, Phys. Rept. **388** (2003) 41.
- [17] J. C. Collins, L. Frankfurt and M. Strikman, Phys. Rev. D **56** (1997) 2982; S. V. Goloskokov and P. Kroll, arXiv:hep-ph/0501242.
- [18] I. P. Ivanov and N. N. Nikolaev, Phys. Rev. D **65** (2002) 054004.
- [19] C. Adloff *et al.* [H1 Collaboration], Eur. Phys. J. C **13** (2000) 371; J. Breitweg *et al.* [ZEUS Collaborations], Eur. Phys. J. C **12** (2000) 393.
- [20] K. Schilling and G. Wolf, Nucl. Phys. B **61** (1973) 381.
- [21] J. M. Link *et al.* [FOCUS Collaboration], Phys. Lett. B **545** (2002) 50.